Analysis and Optimization of Third Order Intermodulation Distortion Mechanisms in AlGaAs/GaAs Heterojunction Bipolar Transistors [1]

Apostolos Samelis and Dimitris Pavlidis

Solid State Electronics Laboratory
Department of Electrical Engineering and Computer Science
The University of Michigan
Ann Arbor, MI 48109-2122

Abstract: **In this paper the third order intermodulation distortion (IMD3) mechanisms of HBT's are analyzed using Volterra Series theory. The third order nonlinear currents generated by the device nonlinearities are evaluated for this purpose. Second harmonic loading is addressed in view of IMD3 optimization while, at the same time, maintaining high gain through conjugate matching at the fundamental frequency. It is shown that IMD3 depends on a complex process involving interactions between various nonlinear elements and is highly sensitive to C_{bc} generated nonlinear current. The interaction of the latter with the other HBT elements significantly impacts the IMD3. Optimum IMD3 occurs at high second harmonic reflection coefficients corresponding to open load conditions. Up to $27\,dBm$ IMD3 improvement can be obtained by proper loading.**

I. Introduction

Heterojunction Bipolar Transistors (HBT's) have demonstrated very low harmonic distortion characteristics with excellent third order intermodulation product intercept point, IP3 [1]. Their intermodulation (IMD3) characteristics have been the subject of recent studies which showed that the good IMD3 performance is due to partial cancellation of the IM currents generated by the resistive emitter junction and those generated by the junction capacitance [2].

Volterra Series has been extensively used as nonlinear analysis tool in the past and it has proved to be very satisfactory for modeling frequency dependent distortion in weakly nonlinear devices [3], [4], [5]. Narayanan followed this approach in order to analyze the nonlinear distortion of BJT's [6] and evaluate the impact of frequency, bias and loading conditions on the intermodulatiopn characteristics. The implementation of Volterra Series in modeling the distortion of bipolar transistors (Si BJT's or HBT's) has been limited due to their inherently strong nonlinear behavior, which confines the dynamic range of calculations in the small signal region. However, it provides the possibility of examining in detail the contribution of each nonlinearity on the IMD3 characteristics through the evaluation of the nonlinear currents generated by them and their possible interactions.

This paper presents a further insight to the nonlinearities of HBT's by investigating the impact of their third order nonlinear currents on IMD3, under various second harmonic and low frequency load conditions. Using the Volterra Series approach, it is shown that IMD3 is minimized under certain loading. This corresponds to the conditions where the third order nonlinear current at the base emitter junction approaches its minimum. The results provide the circuit designer with the capability of optimizing IMD3 through load tuning at frequencies other than the fundamental while maintaining maximum transducer gain through loading under conjugate match conditions at the fundamental frequency.

II. Large Signal Modeling Using Volterra Series

A special HBT modeling procedure was developed for the purpose of (i) calculating the IMD3 characteristics of the HBT, (ii) evaluating the impact of each device element on IMD3 and (iii) providing a fast and efficient calculation of the second harmonic load yielding optimum IMD3. The probing method [7] was used to implement Volterra Series theory. The analysis of the IMD3 meachanisms was made made up to third order approximation.

The input signal exciting the HBT can be described using Volterra Series as follows:

$$v_s(t) = \sum_{i=1}^{K} A_i e^{j\omega_i t}. \qquad (1)$$

If $v_j(t)$ is the voltage at node j, then this voltage can be expressed, to an n-th order approximation, in terms of the m-th order nonlinear transfer functions, $H_{jm}(j\omega_1, j\omega_2, ..., j\omega_m)$ (with $m = 1, 2, 3, ..., n$), as follows:

$$v_j(t) = \sum_{m=1}^{n} v_{jm}(t), \qquad (2)$$

where

[1] This work has been supported by Alcatel-Espace (Contract No. 393/550.760), Bell Northern Research and ARO (Contract No. DAAL 03-87-K-0007)

$$v_{jm}(t) = \sum_{k_1=1}^{K}\sum_{k_2=1}^{K}\cdots\sum_{k_m=1}^{K}\left(\prod_{i=1}^{m} A_{k_i}\right)$$
$$H_{jm}(j\omega_{k_1}, j\omega_{k_2}, ..., j\omega_{k_m})e^{(j\omega_{k_1}t+j\omega_{k_2}t+...+j\omega_{k_m})t}. \quad (3)$$

The calculation of the nonlinear transfer functions is performed sequentially, from lowest to highest order, by solving linear systems of equations. The first order transfer functions determine the response of the linear circuit, while the second or higher order functions account for the device's nonlinear behavior. Nonlinear currents are defined for second or higher order calculations. These are imaginary currents exciting the circuit at the frequencies of the generated harmonics. Second (or third) order currents are proportional to the second (or third) derivative of the charge or current of a particular element with respect to V_{be} or V_{ce}. The second (or third) order nonlinear transfer functions are calculated by solving the linear system corresponding to nonlinear currents of the respective order. This analysis is carried out at the frequency of the harmonic under question.

Given a real input, the fundamental and third order intermodulation voltage at frequency $2\omega_1 - \omega_2$ for node k and to a third order accuracy are given by:

$$v_{k,\omega_1}(t) = \frac{1}{2}B_k e^{j\omega_1 t} + \frac{1}{2}B_k^* e^{-j\omega_1 t} \quad (4)$$

$$v_{k,2\omega_1-\omega_2}(t) = \frac{1}{2}C_k e^{j2\omega_1 t - j\omega_2 t} + \frac{1}{2}C_k^* e^{-j2\omega_1 t + j\omega_2 t} \quad (5)$$

where,

$$B_k = A_1 H_{k1}(j\omega_1) + \frac{3}{4} \mid A_1^2 \mid A_1 H_{k3}(-j\omega_1, j\omega_1, j\omega_1) + \frac{3}{2} \mid A_2^2 \mid A_1 H_{k3}(-j\omega_2, j\omega_1, j\omega_2) \quad (6)$$

and

$$C_k = \frac{3}{4}A_1^2 A_2^* H_{k3}(j\omega_1, j\omega_1, -j\omega_2). \quad (7)$$

Consequently, the power absorbed by the load at the fundamental frequency, ω_1, is given by,

$$P_{out} = \frac{1}{2} \mid B_4 \mid^2 \mid Y_l(j\omega_1) \mid cos[\angle Y_l(j\omega_1)]. \quad (8)$$

Similarly, the power absorbed by the load at the frequency $2\omega_1 - \omega_2$ is the third order intermodulation product (IMD3), given by,

$$P_{IMD3} = \frac{1}{2} \mid C_4 \mid^2 \mid Y_l(j2\omega_1 - j\omega_2) \mid cos[\angle Y_l(j2\omega_1 - j\omega_2)]. \quad (9)$$

Finally, the input power is given by,

$$P_{in} = \frac{1}{2} \mid B_1 \mid^2 \mid Y_{in}(j\omega_1) \mid cos[\angle Y_{in}(j\omega_1)], \quad (10)$$

where Y_{in} is the transistor input admittance seen from port 1.

III. Experimental Characterization and Modeling Procedure

The devices were AlGaAs/GaAs HBT's with a thick $1.5\,\mu m$ n-GaAs collector intended for power applications. Load Pull measurements were performed under single and double tone excitation with signals at frequencies $f_1 = 8\,GHz$ and $f_2 = f_1 + \Delta f$, where $\Delta f = 100\,kHz$. DC bias was selected for Class-AB operation. The source impedance was set close to its simultaneous match value to assure maximum gain. The Hybrid-π model, shown in Figure 1, was used for device simulations. Multibias tests and equivalent circuit extractions permitted the evaluation of the base current (I_B) and collector-emitter voltage (V_{CE}) dependence of all circuit parameters considered to be nonlinear (i.e. C_{je}, g_{je}, C_{bc} and g_m). Figure 2 shows the bias dependence of g_m. All S-parameters were measured over the frequency range of 1.5 to $26.5\,GHz$. To validate the modeling approach followed here, the Third Order Intercept Point (IP3) was obtained from the theoretical and measured output power. The discrepancy between the measured and modeled IP3 was of the order of $1\,dB$.

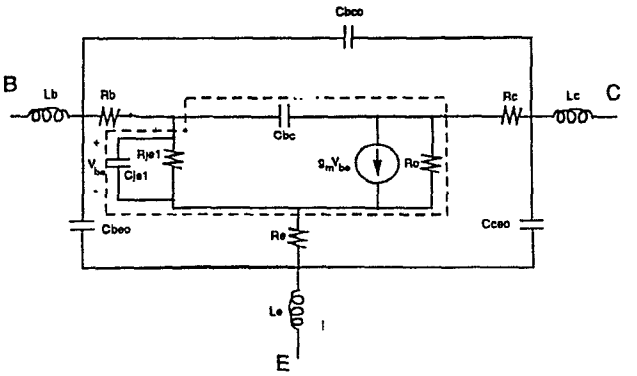

Figure 1: Large Signal Model Used for the HBT

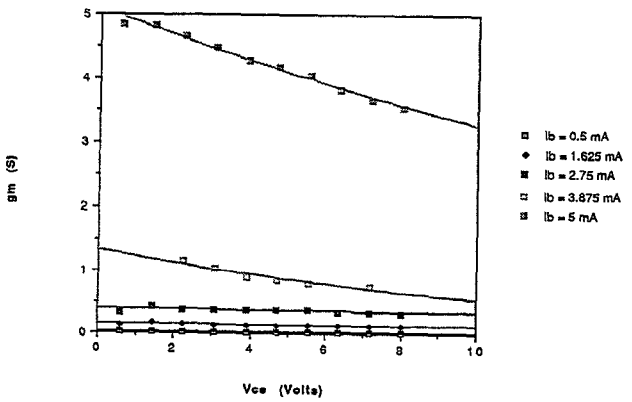

Figure 2: g_m Bias Dependence of the HBT

IV. Modeling and Optimization of HBT IMD3 Behavior Through Third Order Nonlinear Current Evaluation

Optimum output power and IMD3 performance can be controled simultaneously by adjusting the effects of the various nonlinearities according to variable external load conditions in order to obtain: (i) conjugately matched conditions

at the fundamental frequency for maximum gain and (ii) proper second harmonic termination for low IMD3 product. Both conditions are possible by selecting appropriate load (Y_l) frequency responses so that $Y_l(f_1)$ satisfies best the gain requirement while, $Y_l(2f_1)$ (at the second harmonic frequency) provides low IMD3. The analysis presented here is performed for various $Y_l(2f_1)$ values corresponding to different load reflection coefficient magnitude ($G_{l,2f,mag}$) and phase ($G_{l,2f,ph}$).

The contribution and impact of the model's nonlinear elements on IMD3, can be determined by examining the third order nonlinear currents generated by each element at frequency $2f_1 - f_2$. The nonlinear third order currents were investigated as function of the load at the second harmonic frequency. Y_l and Y_s where set equal to $1/50\,S$ at DC while at the fundamental frequency they where set close to the conjugate match value of the devices.

Figure 3 shows the third order nonlinear currents generated by the four nonlinearities as a function of the phase of the load reflection coefficient, $G_{l,2f,ph}$ at a magnitude equal to $G_{l,2f,mag} = 0.55$. All currents where evaluated at an input power level of $-10\,dBm$. Included in this figure are also the sums of the currents generated by g_{je} and C_{je} (indicated as $g_{je} + C_{je}$), the sum of the currents generated by g_{je}, C_{je} and C_{bc} together, indicated as $g_{je} + C_{je} + C_{bc}$ and the difference of the currents generated by C_{bc} and g_m, denoted as $C_{bc} - g_m$. $g_{je} + C_{je} + C_{bc}$ is the total third order nonlinear current entering the input base terminal, while $C_{bc} - g_m$ is the total current entering the output collector node. This approach allows one to investigate the importance of each element and the interactions between each other. As one notices, the nonlinear current generated by C_{je} turns out to be the strongest of all elements followed by the transconductance, g_m. The g_{je} and C_{bc} related nonlinear currents were lower than that of C_{je}. The observed trends will be discussed next with the help of the results of Figure 4.

Figure 4 shows the corresponding phases of all nonlinear currents discussed above. Nonlinear current cancellation between currents entering a node occurs at the the point where the phase difference of the participating elements is greater than $\pi/2$. In Figure 4 one notices such a difference between the C_{je} and g_{je} generated currents. However, for the particular device operating conditions, the sum of the C_{je} and g_{je} generated nonlinear currents is only marginally lower than the C_{je} generated current due to the small contribution of g_{je} (Figure 3). At different bias or frequency conditions g_{je} and C_{je} may, however, show a more pronounced cancelling effect. These observations are not an absolute criterion for determining the degree of device nonlinearity; it turns out from the results below that IMD3 is after all depending to some extent on C_{je} and g_{je} interaction. Furthermore, the phase difference between $C_{je} + g_{je}$ and C_{bc} currents is smaller than $\pi/2$, which implies a total base current due to $C_{je} + g_{je} + C_{bc}$ higher than that due to the $C_{je} + g_{je}$ current alone. This is also confirmed by the results of Figure 3. Similarly, at the output node, the total current due to $C_{bc} - g_m$ is higher than the current generated by g_m alone due

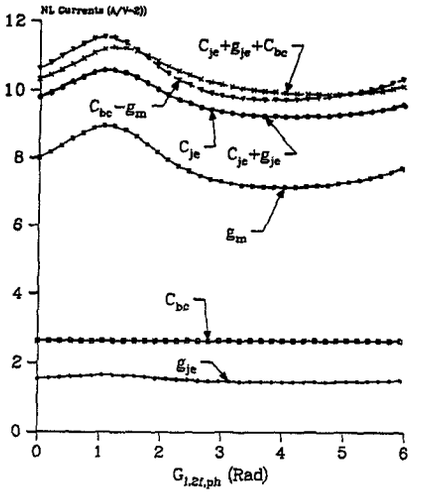

Figure 3: Third Order Nonlinear Current Magnitudes vs. the Phase, $G_{l,2f,ph}$, of the Second Harmonic Load at $G_{l,2f,mag} = 0.55$

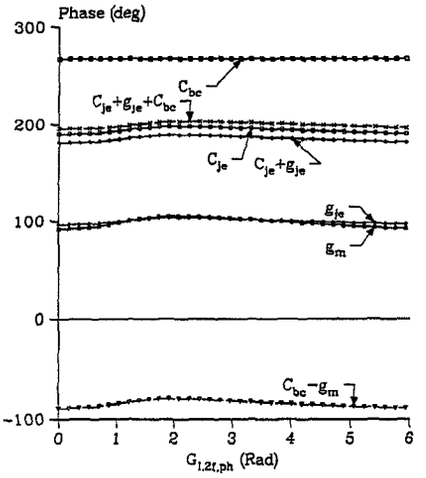

Figure 4: Third Order Nonlinear Current Phases vs. the Phase, $G_{l,2f,ph}$, of the Second Harmonic Load at $G_{l,2f,mag} = 0.55$

to the larger than $\pi/2$ phase difference between these current components. It is concluded therefore that, although C_{bc} generates a weaker current, compared to C_{je} and g_m, its interaction with these elements results in more pronounced nonlinear characteristics.

The contribution of each element and its importance on IMD3 can be evaluated by comparing the IMD3 value when all nonlinearities are present with its value when the third order nonlinear current of a particular element is eliminated. Figure 5 shows IMD3 characteristics under $G_{l,2f,mag} = 0.75$ termination conditions when all elements are present, as well as, when the nonlinear currents due to particular elements or combination of them are eliminated. As one notices, IMD3 is highly sensitive to C_{bc} related nonlinear current; absense of this current component would improve IMD3 by at least 10 dBm. Furthermore, the presence of the nonlinearities due to C_{je}, g_{je} and g_m together improves IMD3. The in-

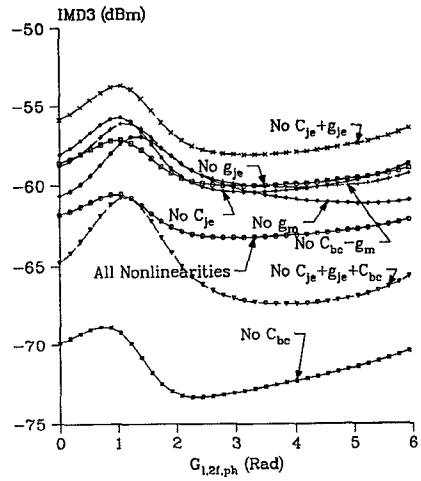

Figure 5: Sensitivity of IMD3 on Third Order Currents Due to Various Device Nonlinearities

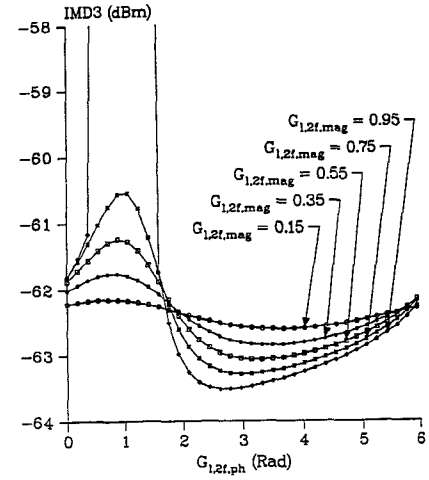

Figure 6: IMD3 vs. $G_{l,2f,ph}$ for various $G_{l,2f,mag}$

teraction between C_{bc} and g_m results in improved IMD3; IMD3 is degraded if this interaction, which is in the form of $C_{bc} - g_m$ related current, is ignored. The interaction between C_{bc} and C_{je}, g_{je} results in IMD3 degradation; when the currents related to $C_{je}+g_{je}+C_{bc}$ interactions are ignored then IMD3 is improved. Finally, the interaction between C_{je} and g_{je} results in IMD3 improvement as already discussed by others [2]. Overall, one notices that the way IMD3 is determined depends on a complex process which involves interactions between nonlinear currents of different nature.

As discussed next, the choise of the second harmonic load is important in order to fully optimize the IMD3 characteristics. Figure 6 shows IMD3 vs. $G_{l,2f,ph}$ at an input power of $-10\ dBm$ for various second harmonic load reflection coefficients, $G_{l,2f,mag}$. It is obvious that best IMD3 requires high reflection coefficients having phases at the open load region of the Smith chart. The lowest and highest IMD3 values are determined by the interaction between the input (base) and output (collector) node nonlinear currents. Comparison between the results of Figures 3 and 6 shows that, worst IMD3 occurs at a $G_{l,2f,ph}$ corresponding to the maximum of the $C_{je} + g_{je} + C_{bc}$ and $C_{bc} - g_m$ related currents while best IMD3 is closer to the minimum of these currents. The improvement of IMD3 for various second harmonic loads can be up to 27 dBm if one compares the extreme cases corresponding to these nonlinear currents under very large output reflection coefficients (i.e. $G_{l,2f,mag} = 0.95$ of Figure 6).

V. Conclusion

The IMD3 performance of HBT's was studied using a generalized Volterra Series approach, which allows device analysis under variable second harmonic load conditions. The mechanisms dominating IMD3 are determined by the nonlinear current entering the base junction. C_{je} is the strongest nonlinearity of the device. C_{bc} is the most important element contributing in IMD3. Its interaction with the rest of the elements either improves IMD3 (in the presence for example of $C_{bc} - g_m$ third order currents) or degrades it (i.e. in the presence of $C_{je} + g_{je} + C_{bc}$ currents). IMD3 can be optimized by selecting the load at the second harmonic at the point where the total base and collector nonlinear current are close to their minimum, i.e. close to open load conditions ($G_{l,DC,ph} = 3.14\ Rad$).

VI. Acknowledgments

The authors would like to thank Doug Teeter, Phil Marsh and Marcel Tutt for providing help during device characterization.

References

[1] M.E. Kim et. al., "12–40 GHz Low Harmonic Distortion And Phase Noise Performance Of GaAs HBTs", GaAs IC Symposium 1988, pp. 117–120.

[2] S.A. Maas, B. Nelson, D. Tait, "Intermodulation in Heterojunction Bipolar Transistors", 1991 IEEE MTT-S Digest, pp. 91-93.

[3] S.A. Maas, D. Neilson, "Modeling MESFET's for Intermodulation Analysis of Mixers and Amplifiers", IEEE Transactions on MTT, Vol. 38, No. 12, Dec. 1990, pp. 1964-1971.

[4] R.A Minasian, "Intermodulation Distortion Analysis Of MESFET Amplifiers Using The Volterra Series Representation", IEEE Trans. on MTT, vol. MTT-28, No.1, Jan. 1980, pp. 1-8.

[5] G.M. Lambrianou, C.S. Aitchison, "Optimization of Third-Order Intermodulation Product and Output Power from an X-Band MESFET Amplifier Using Volterra Series Analysis", Transactions on MTT, Vol. MTT-33, No 12, Dec. 1985, pp. 1395-1403.

[6] S. Narayanan, "Transistor Distortion Analysis Using Volterra Series Representation", Bell System Technical Journal, May-June 1967, pp. 991-1024.

[7] J. J. Bussgang, L. Ehrman, J. W. Graham, "Analysis of Nonlinear Systems with Multiple Inputs", Proc. of the IEEE, vol. 62, No. 8, August 1974, pp. 1088-1119.